Techno-economic analysis and comparison of an ORC-VCC biomass-solar hybrid trigeneration system and a PV driven heat pump

K. Braimakis[a], T. Roumpedakis[b], A.Thimo[c] and S.Karellas[d]

[a] *National Technical University of Athens, Athens, Greece, mpraim@central.ntua.gr,*
[b] *National Technical University of Athens, Athens, Greece, roumpedakis_t@hotmail.com*
[c] *National Technical University of Athens, Athens, Greece, antzelath@central.ntua.gr*
[d] *National Technical University of Athens, Athens, Greece, sotokar@mail.ntua.gr*

Abstract: Every year a great deal of energy is consumed for meeting the heating and cooling demands in houses and utility buildings. Meanwhile, the policies adopted worldwide aiming at the reduction of CO_2 emissions and the consumption of fossil fuels have led to the study and the development of technological solutions based on the use of renewable energy sources such as biomass and solar power for heating and cooling purposes. In this study, the implementation of a micro-scale trigeneration (heating, cooling and electricity) ORC-VCC system incorporating a biomass boiler and a series of solar thermal collectors is technically and economically analyzed and evaluated against a heat pump powered by photovoltaic panels. The operation of both systems is modeled thermodynamically and simulated by considering the heating and cooling loads of a typical building located in the island of Crete, Greece. An economic analysis is subsequently carried out considering all relevant investment and operating costs. The aforementioned systems are economically assessed against a traditional heating and cooling configuration consisting of a natural gas boiler and a conventional heat pump in order to thoroughly estimate and display the potential economic savings of each technological application.

Keywords:
Biomass, Heat Pump, solar. Techno-economic analysis, Trigeneration, Organic Rankine Cycle.

1. Introduction

In the recent years, a lot of interest has been focused on multigeneration systems, which aim to convert an energy source (fossil, solar, waste heat) into combined electricity, cooling and heating. This is justified by the fact that the traditional electricity production systems have a limited efficiency (around 30-40 [1], [2] %), so a great deal of the primary heat ends up being rejected unexploited to the environment in the form of waste heat. Due to the policies followed worldwide in order to increase overall system efficiencies and decrease greenhouse gas (GHGs) emissions, a lot of research has been carried out on cost competitive co-generation and combined cooling heating and power systems. Furthermore, such small scale multigeneration systems that use renewable energy sources have gathered significant attention, since they can contribute to further reducing emissions and ensuring sustainability and fuel independence, while at the same time constituting a driving force for economic development. In this study two trigeneration systems are thermodynamically simulated and economically evaluated and compared against conventional heating (oil boiler and commercial heat pump). The systems consist of a) an Organic Rankine Cycle (ORC) interconnected with a Vapor Compression Cycle (VCC) that uses solar-thermal parabolic trough collectors (PTC) and a biomass boiler and b) a photovoltaic-powered heat pump. The two systems are capable of combined electricity, cooling and heating generation.

2. Hybrid Solar-ORC-VCC system [3]

2.1. Description of the system

The hybrid Solar-ORC-VCC system consists of a biomass boiler, parabolic trough collectors and an ORC which is interconnected to a heat pump (Fig. 1).

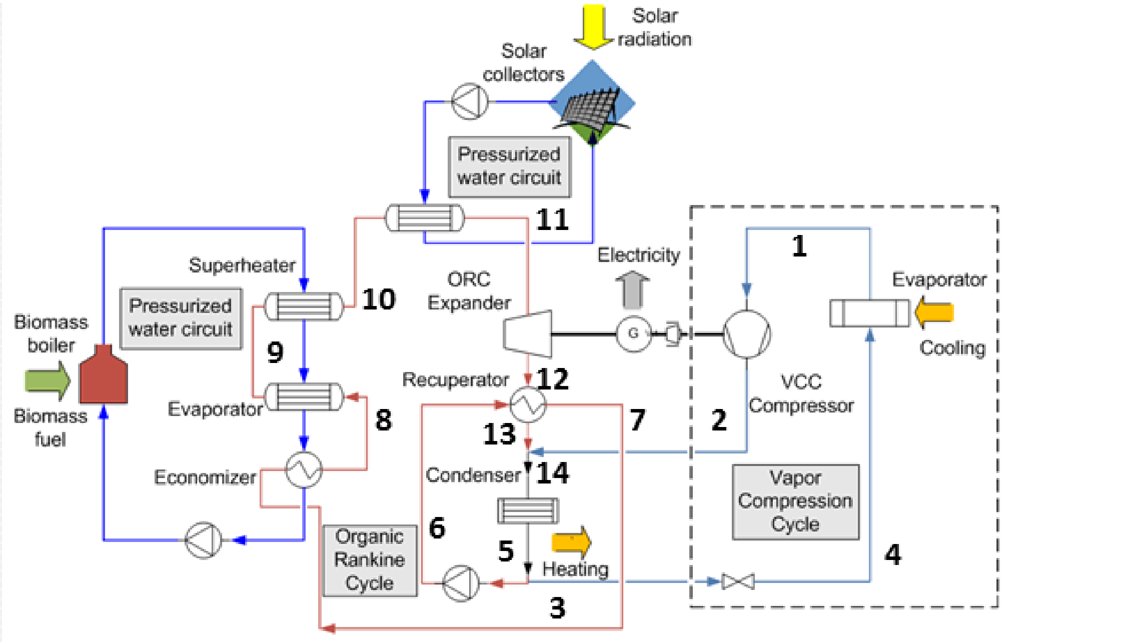

Fig. 1. Solar ORC- heat pump system, biomass boiler and PTC circuits.

The ORC configuration includes a pump, an expander, a condenser and heat exchangers for the transfer of heat from the biomass boiler and the PTC circuit to the working fluid. The heat is mainly provided by the PTC circuit and secondarily, when solar thermal energy is inadequate, by the biomass boiler circuit. Both circuits use pressurized water for the thermal transfer. The pressure of water is kept at high levels, in order to keep it in a liquid state.

During the winter (cogeneration mode), the heat pump is not operational. The operation of the ORC is adjusted so that the condensation heat balances the thermal demand (space heating and DHW (Domestic Hot Water)). The power produced by the expander is converted to electricity through a generator and is used to power the circulating pump, while the power in excess is sold to the grid.

During the summer (trigeneration mode**)**, when cooling is required, the ORC and the heat pump are interconnected. The steam exiting the expander is mixed with the stream coming from the VCC compressor. In this mode, a scenario of following the cooling load is assumed. The required cooling is produced during the evaporation process in the heat pump. The electricity produced from the ORC generator should be such that it can supply the circulating pump and the VCC compressor. There is thus no excess electricity to be sold to the grid in the trigeneration mode.

The technical characteristics of the units that compose the system are given in the Table 1 below.

Table 1. PTC- ORC-VCC technical characteristics

Biomass boiler	*PTC[4]*	*Heat Exchangers*	*Other assumptions*
Maximum load =30 kW_{th}	Type: PTC-1000	Pinch point: 5-10 K	Pump isentropic efficiency=65%
Maximum water temperature=110 °C	Rotation axis=absorber tube axis Size: 1x 2 m^2		Scroll expander isentropic efficiency=60%
HHV=17000 kJ/kg	Operating temperature: 120 -200 °C		Compressor isentropic efficiency=75%
Boiler efficiency=82,88 %	Efficiency parameters: η_0=0,70 a_1= 0,2044 W/(m^2K) a_2=0,001545 W/ (m^2K^2) Total surface: 32 m^2		Generator efficiency=85% Mechanical efficiency= 98% Electric motor efficiency=85%

2.2. System performance

The system was simulated in Matlab, while the thermodynamic values at each point of the ORC-VCC cycle were extracted from Coolprop database. A steady state of operation is assumed, while all pressure drops and heat losses are neglected.

The organic fluid used in both the ORC and the heat pump is R227ea, which is commercially suitable for air conditioning systems, heat pumps and thermal collectors.

Due to the restriction with regard to the maximum water temperature of the biomass boiler, the working fluid will be superheated by the parabolic trough collector's circuit up to the temperature of 110 °C, while the pressure will be kept at a level above the supercritical pressure (supercritical ORC). According to thermodynamic investigations for the optimization of the system (in order to maximize thermal efficiency of ORC (η_{th_orc}), COP_{vcc} (Coefficient of Performance) and electrical efficiency (η_{el})), it has been found that the optimum pressure of the organic medium after the circulating pump (point 6), is 30.4 bar. The condensation temperature is set to 50°C (for cooling and heating mode) in order to get the required temperature for the covering the heating demand (45°C).

2.2.1. System performance in heating mode

The scenario assumed on heating mode (following thermal load) is described by the following equations:

$$m_{ORC}(i) = \frac{Q_{th\_load}(i)}{h(10) - h(11)}, \quad i = 1:4 \ \text{and} \ i = 11:12 \ (\text{for heating period months}) \qquad (1)$$

The heat provided by the PTC system is equal to:

$$Q_{sol}(i) = m_{ORC}(i) \cdot (h(8) - h7(i)) \qquad (2)$$

And the heat provided by the biomass boiler circuit is:

$$Q_{bio}(i) = m_{ORC}(i) \cdot (h7(i) - h(6)) \qquad (3)$$

The heat input to the system via the boiler circuit (biomass consumption) will vary per month, depending on the heat provided by the PTC circuit (solar radiation) and the mass flow rate of the working fluid.

Table 2. PTC-ORC-heat pump thermodynamic state points in heating mode

Point	***5***	***6***	***8***	***9***	***10***	***11***	***12***
p(bar)	9.16	30.40	30.40	9.16	9.16	9.16	9.16
T (°C)	50.00	52.43	110.00	68.73	68.73	50.00	50.00
h(kJ/kg)	56.0637	58.6132	179.6592	170.4300	170.4300	56.0637	56.0637

All points of the thermodynamic cycle will remain constant at the heating mode operation, apart from point 7, whose temperature is varied by fluctuating the mass flow rate of the pressurized water in the biomass boiler circuit. At this point, a minimum temperature equal to the temperature of point 6 has been set (assuming no operation of the biomass boiler circuit).

Table 3. PTC-ORC-heat pump point 7 in heating mode

p (bar)	30.40
T (°C)	52.43 – 103.76

For the months only with DHW load (May and October) a minimum mass flow rate that corresponds to the minimum temperature of point 7, has been assumed.

2.2.2. System performance in cooling mode

The evaporation temperature depends on the desired cooling temperature. The COP of the heat pump increases with the evaporation temperature. Taking into account the pinch point temperature difference of the heat exchangers, the evaporation temperature will be set equal to 7 °C. The heat pump includes no superheating or subcooling of the working fluid.

The scenario assumed in cooling mode (following cooling load) is described by the following equations:

$$m_{VCC}(i) = \frac{Q_{c\_load}(i)}{h(1) - h(4)}, \quad i = 6:9 \, (\text{cooling period}) \qquad (4)$$

The mass flow rate of the ORC is defined by the power balance equation, which implies that the power produced during the expansion process is equal to the power consumed by the ORC-pump and the VCC-compressor.

$$P_{exp,ORC} = P_{comp,VCC} + P_{pump,ORC} \qquad (5)$$

During this period, the heat produced in the condenser is greater than the heat required for the DHW. The heat in excess is rejected to the environment.

The thermodynamic state points in cooling mode are presented in Table 4 and 5. Points 5, 6, 8, 9, 11, 12 of the cycle, preserve the same values as in the heating mode.

Table 4. PTC-ORC-VCC thermodynamic state points in cooling mode

Point	***1***	***2***	***3***	***4***	***10***
p(bar)	2.52	9.16	9.16	2.52	9.16
T (°C)	7.00	50.00	50.00	7.00	62.71
h(kJ/kg)	125.6651	146.2232	56.0637	56.0637	164.4937

Table 5. PTC-ORC-VCC point 7 in cooling mode

P(bar)	30.40
T (°C)	103.44 – 103.91

The overall system efficiency in heating and cooling mode, respectively, is expressed by the following equations:

$$\eta_{tot,heating} = \frac{Q_{th\_load} + P_{el}}{\frac{Q_{bio}}{\eta_{bio}} + \frac{Q_{sol}}{\eta_{PTC}}} \quad (6) \qquad \eta_{tot,cooling} = \frac{Q_{th\_DHW} + Q_{c\_load}}{\frac{Q_{bio}}{\eta_{bio}} + \frac{Q_{sol}}{\eta_{PTC}}} \quad (7)$$

The annual operation variables of the system are listed into the following table.

Table 6. Annual operational variables of PTC-ORC-heat pump

m_{orc}(kg/s)	0.05 - 0.307
m_{VCC}(kg/s)	0.064 - 0.0999
η_{tot} (%)	18.9-69.22
η_{el} (%)	3.87
COP_{VCC}	3.39
P_{elsell} (kWh_e/y)	1330.51
Q_{bio} (kW_{th})	0-29.8
m_{bio} (kg/s)	0-0.0021

3. PV –heat pump system

3.1. Description of the system

Due to its efficiency, simplicity and reliability, the solar Vapor Compression refrigeration is believed to be the most competitive and cost effective solution for the residential sector (Immovilli et al. [5]) and especially in subtropical climates (Fong et al. [6]). The potential of a solar trigeneration system has been also proved by Joyce et al [7], who studied a PV/T and heat pump based trigeneration system located in a dwelling in Lisbon, Portugal.

The PV-heat pump configuration includes the photovoltaic (PV) circuit (PV modules and inverter), an evaporator, a condenser, a compressor and a throttle valve (Fig. 2). The heating is produced through the condensation process while the cooling is obtained during the evaporation process. Thus, the heat pumps are reversible vapor compression devices operating efficiently in both directions.

This system was also simulated in Matlab and the thermodynamic values were calculated from Coolprop. The working fluid used in the heat pump system is R227ea.

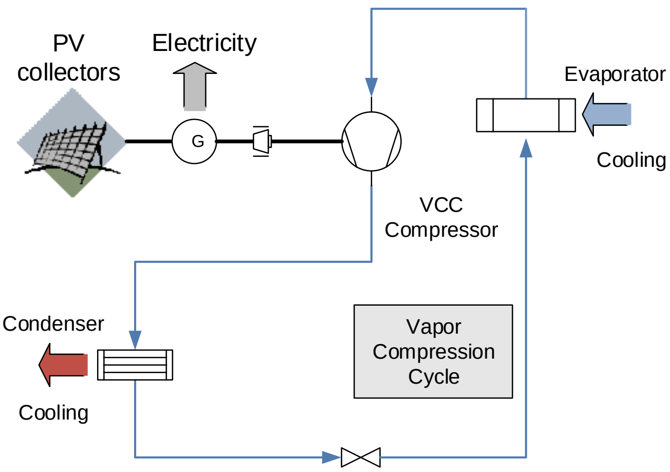

Fig.2. PV- heat pump system

3.1.1. PV circuit

The photovoltaic panel, chosen for this specific study, is Panasonic N240 HIT (Heterojunction with Intrinsic Thin layer [8-9]). The solar cell is made of a thin monocrystalline silicon wafer surrounded by ultra-thin amorphous silicon layers and can maintain high efficiency at high temperatures.

*Table 7. PV technical characteristics**

Type	Panasonic HIT N240
Size	0.798 mm x 1580 mm
Module efficiency	19 %
Output/m²	190 W/m^2
Max. power (Pmax) (W)	240
Max. power voltage (V)	43.7
Max. power current (I)	5.51

* Note: At Standard Test Conditions: Air mass 1.5; Irradiance =1000 W/m^2; cell temp. 25°*C*

The efficiency of the PV modules has been estimated taking into account the cell temperature, the effect of the irradiance and by using a correction factor to account for air pollution. The behavior of PV modules has been assumed linear with regard to irradiance, considering a maximum power point operation and considering that the MPPT voltage remains relatively constant while the current flowing through the panels decreases together with the irradiance. The PV system has been sized for the worst-case scenario energy demand, which is on January and concerns thermal load (space heating and DHW). For a COP equal to 3.85 (as calculated on January) the maximum required power of the PV system, is 12 kW_e. The total PV module area is 65.56 m^2 (52 PV modules). The PV modules exhibit an average annual electric efficiency of 16.29 %. The efficiency factor of the MPPT-inverter and the electric losses due to cabling and connection to the network, were considered 95 % and 5 %, respectively.

3.1.2. Heat pump

The operation of heat pump (HP) units is based on the Vapor Compression Cycle (a reversible Rankine thermodynamic cycle) and includes the transfer of heat from a cold to a hotter environment, with the use of work, provided by the compressor.

The compressor, powered by an electric motor, compresses the working fluid while the throttle valve aims at its isenthalpic expansion without producing any power.

The efficiency of the heat pump in each operating mode is evaluated by the following indicators:

$$COP_{heat}(k) = \frac{Q_{th\_load}(k)}{P_{comp}(k)}, \quad k = 1:5 \text{ and } k = 10:12 \text{ (heating period)} \quad (8)$$

$$COP_{cool}(k) = \frac{Q_{c\_load}(k)}{P_{comp}(k)}, \quad k = 6:9 \text{ (cooling period)} \quad (9)$$

3.2. System performance

In this study a grid-connected system has been assumed. The photovoltaic system is connected to an MPPT device –inverter (dc/ac) and the electricity production is used to supply the motor driving the compressor of the heat pump, when solar power is available. The heat produced is either consumed or stored in a TST (Thermal Storage Tank). When solar power is not available, the heat pump is supplied with power from the grid and accordingly when electricity is produced in excess it is sold to the grid. The PV-HP system can be considered as a **trigeneration** or **cogeneration** system only when solar power is available and adequate to supply the compressor in cooling or heating period, respectively.

The calculations have been carried out based on the following assumptions.

Table 8. PV- Heat Pump Assumptions

Pinch point (condenser- evaporator)	5-10 K
Compressor isentropic efficiency (%)	75
Mechanical efficiency (%)	98
Electric motor efficiency (%)	85

The evaporation temperature in heating mode is equal to the ambient temperature increased by the pinch point (10 K) of the evaporator while in cooling mode is set 7 °C. The condensation temperature is 50 °C.

The scenarios assumed in **heating mode (**following thermal load) and **cooling mode** (following cooling load) are described by the following equations:

$$m_{VCC}(k) = \frac{Q_{th\_load}(k)}{h(2,k) - h(3)}, \quad k = 1:5 \text{ and } k = 10:12 \text{ (heating period)} \quad (10)$$

$$m_{VCC}(k) = \frac{Q_{c\_load}(k)}{h(1,k) - h(4)}, \quad k = 6:9 \text{ (cooling period)} \quad (11)$$

The heat produced during the cooling period at the condenser is greater than the one needed for DHW. The heat in excess is rejected to the environment, similarly to the case of the solar-ORC-heat pump system.

The annual operational variables and the thermodynamic state points of the PV-HP system are displayed in the following tables.

Table 9. PV-HP operational variables

m_{vcc} *(kg/s)*	0.038-0.211
COP_{cool}	3.39
COP_{heat}	1.39 – 4.82

Table 10. PV-HP thermodynamic state points in heating mode

Point	***1***	***2***	***3***	***4***
p(bar)	2.11- 2.82	9.16	9.16	2.11- 2.82
T (°C)	2.1-10.3	50	50	2.1-10.3
Phase	Saturated vapor	Saturated vapor	Saturated liquid	Saturated liquid

Table 11. PV-HP thermodynamic state points in cooling mode

Point	***1***	***2***	***3***	***4***
p(bar)	2.52	9.16	9.16	2.52
T (°C)	7	50	50	7
Phase	Saturated vapor	Saturated vapor	Saturated liquid	Saturated liquid

The monthly heating and cooling load as well as the electricity purchased or sold (depending on the system balance) are shown in Fig.3.

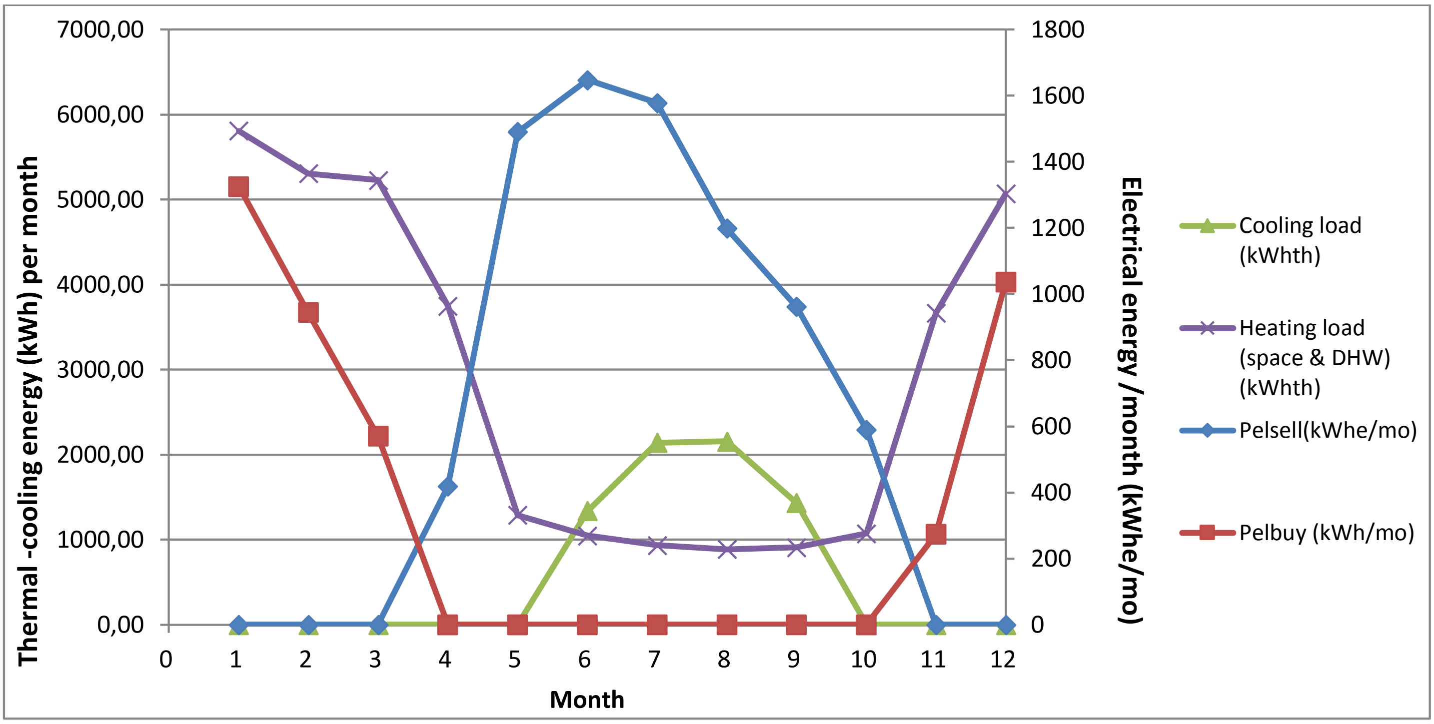

Fig.3. Energy produced/consumed per month in PV- HP system

4. Climate model parameters and meteorological data

The heating and cooling systems under evaluation are assumed to be installed in a newly constructed Greek apartment block, located in Heraklion in Crete. Heraklion is located at 35°20′N and 25°11′E and has a Subtropical-Mediterranean climate. Summers are warm to hot and dry with clear skies while winters are mild with moderate rain. The desired indoor environmental conditions for the building considered are given in Table 12 [10].

Table 12. Desired indoor conditions

Heating period	November-April
Cooling period	June-September
Average indoor heating temperature	20 °C
Average indoor cooling temperature	26 °C
Average winter indoor relative humidity	40%
Average summer indoor relative humidity	45%
Required fresh air	0.75 $m^3/h/m^2$
Annual consumption of hot water	50 lt/person/day
Average DHW temperature	45 °C

The DNI (Direct Normal Insolation) data were calculated based on the average monthly total and diffuse solar radiation on a horizontal plane values provided by the Technical Chamber of Greece [11]. Assuming a representative day for each month, and beginning from the sunrise to the sunset time, the hourly total, diffuse and direct radiation has been calculated [12-14].

5. Cooling and heating load

Assuming complete exterior insulation of the building, no basement, no boiler room, no adjacent buildings or balconies (no shading), double-glazing windows and doors of low heat transfer coefficient, the average heat transfer coefficient U_m (W/m^2K) of the building has been calculated in accordance with the existent Greek legislation [10,15].

Table 13. Characteristics of the building

Number of floors	3
Number of apartments/floor	2
Apartment area	105 m^2
Number or persons/apartment	4
Building volume	2560 m^3
Average heat transfer coefficient	0.4534 W/m^2K

The heating load of the building consists of the space heating and the hot water demand. For the calculation of the heating and cooling load [16], the method of heating degree days (HDD, base temperature 20°C) and of cooling degree hours (CDH, base temperature 26°C) has been used. The losses [10] of the distribution network and of the terminal units (fan coils, radiators) have been taken into account.

Each system: Biomass-ORC-HP, PV-HP, conventional HHO (Home Heating Oil) boiler operates for approximately 10 hours daily and is provided with water storage tanks aiming at a low cost and flexible operation when solar power is not available.

6. Economic evaluation

The aforementioned systems are economically assessed against a traditional heating and cooling configuration consisting of an oil-fired boiler and a conventional heat pump in order to display the potential economic savings of each technological application.

For a more "fair" evaluation, the price of the electricity sold to the grid was considered equal to the price of electricity bought from the grid. Of course, this may not be always the case, since there can be differences depending on the national legislation which usually aims to promote multi-generational or renewable-based technologies. However, in order to maintain a more generic aspect of the study, this assumption was made. Therefore, the electricity price was considered equal to the average price of electricity of year 2013 in European countries [17].

Table 14. Assumptions for fuel costs [3],[17-18]

Component	*Cost/unit*
Electricity (from grid) COP for conventional HP=3[10] Boiler Efficiency=0.9 [10]	0.168 €/kWh_e
HHO	0.175 €/kWh_{th}
Biomass fuel	200 €/tn

With regard to capital and maintenance cost for the ORC system, due to the lack of commercially available small-scale ORC systems, their prices have been taken from various studies [3], [19-21].

Table 15. Capital, maintenance and operation cost of the PTC-ORC-VCC system

Component	*Cost/unit*	*Total cost (€)*
Woodchips boiler(30kW_{th})	300 €/kW_{th}	9000
PTC[15]	400 €/m^2	12800
ORC module (2.4 kW_e)	2500 €/kW_e	6000
VCC	500 €/kW_{th}	3475
Total Capital Investment Cost		**31275**
Annual maintenance cost		400
Annual operation cost		2600

Table 16. Capital, maintenance and operation cost of the PV-HP system [22-23]

Component	*Cost/unit*	*Total cost (€)*
PV panels	300 €/panel	15600
Inverter (12 kW_e)		3000
Heat pump		10000
FCU (Fan Coil Unit)	250 €/unit	3000
Total capital investment cost		**31600**
Annual maintenance cost		200
Operating cost		700

Calculating the revenue from the electrical energy sold, the annual revenue from the cost avoided for the heat production by the conventional system, the annual revenue from the cost avoided for the cooling load production, the annual revenue from the cost avoided for the annual maintenance of the conventional system, and with a project life of 20 years and an interest rate of 8%, the Net Present Value, the Internal Rate of Return and the Discounted Pay Back Period for each system have been calculated and presented in the table below for each system.

Table 17. NPV, IRR and DBP values for each system

	PTC-ORC-VCC	*PV- HP*
NPV	13008.9 €	44095.65 €
IRR	13 %	24 %
DBP	10.51 y	5.16 y

7. Conclusions

In this study two different heating and cooling systems, have been simulated and economically evaluated in accordance with indicators such as NPV and IRR. Our results have verified that the most cost effective cooling and heating technology in residential buildings is the photovoltaic driven heat pump. With regard to their capital investment cost, it is almost the same. However what makes the ORC technology less economic, is the high operation cost, i.e. the biomass fuel cost.

Acknowledgments

The work presented in this paper has been funded by the Greek State Scholarships Foundation (IKY), Fellowships of Excellence for Postgraduate Studies in Greece - Siemens Program.

Nomenclature

COP Coefficient of performance

DHW Domestic Hot Water

DNI Direct Normal Insolation, W/m^2

FCU Fan Coil Unit

HHO Home Heating Oil

HHV Higher Heating Value, kJ/kg

h specific enthalpy, kJ/kg

m mass flow rate, kg/s

MPPT Maximum Power Point

ORC Organic Rankine Cycle

p pressure, bar

P electric power, kW_e

PTC Parabolic Trough Collectors

PV Photovoltaic

Q thermal or cooling power, kW_{th}

T temperature, °C

U_m average heat transfer coefficient, $W/(m^2\ K)$

VCC Vapour Compression Cycle

Greek symbols

η efficiency

Subscripts and superscripts

el electric

th thermal

c cooling

sol solar

bio biomass

tot total

elsell electricity to sell

exp expander

comp compressor

References

[1] Cho H, Mago PJ, Luck R, Chamra LM. Evaluation of CCHP systems performance based on operational cost, primary energy consumption, and carbon dioxide emission by utilizing an optimal operation scheme. Applied Energy. 2009;86(12):2540-9.

[2] Martins LN, Fábrega FM, d'Angelo JVH. Thermodynamic Performance Investigation of a Trigeneration Cycle Considering the Influence of Operational Variables. Procedia Engineering. 2012;42(0):1879-88.

[3] S. Karellas, K. Braimakis. Energy-exergy analysis and economic investigation of a cogeneration and trigeneration ORC-VCC hybrid system utilizing biomass fuel and solar power. 27st International Conference on Efficiency, 2014.

[4] W. Werner, AEE INTEC and M. Rommel, Fraunhofer ISE. Process Heat Collectors. State of the ART within Task 33/IV.

[5] F. Immovilli, A. Bellini, C. Bianchini and G. Franceschini. Solar Trigeneration for Residential Applications, a Feasible Alternative to Traditional Micro-Cogeneration and Trigeneration Plants. IEEE Industry Applications Society, 2008.

[6] K.F. Fong*, T.T. Chow, C.K. Lee, Z. Lin, L.S. Chan. Comparative study of different solar cooling systems for buildings in subtropical city. Solar Energy, 84, 227 (2010).

[7] A. Joyce, L. Coelho, J. Martins, N. Tavares, R. Pereira and P. Magalhães. A PV / T AND HEAT PUMP BASED TRIGENERATION SYSTEM. 2010.

[8] G. Hahn, S. Joos. Advances in Photovoltaics: Part 3, State-of-the-Art Industrial Crystalline Silicon Solar Cells, 2014.

[9] M. H. Vishkasougheh, B. Tunaboylu. Simulation of high efficiency silicon solar cells with a hetero-junction microcrystalline intrinsic thin layer. Energy Conversion and Management, 2013,72, 141-146.

[10] Analytical national parameter standards for the estimation of the energy efficiency of buildings and the certification of energy efficiency. Athens: Technical Chamber of Greece;2012.

[11] Climatic Data of Greek Areas. Athens: Technical Chamber of Greece; 2012.

[12] Collares-Pereira, M. and A. Rabl. The average distribution of solar radiation – correlations between diffuse and hemispherical and between daily and hourly insolation values. Solar Energy, 22 ,155 (1979)

[13] Liu, B.Y.H. and R.C. Jordan. Daily insolation on surfaces tilted toward and equator. ASHRAE Journal,3(10), 53 (1962).

[14] Klein, S.A. . Calculation of monthly average insolation on tilted surfaces. Solar Energy, 19, 325 (1977).

[15] Thermophysical properties of building materials and control of building thermal insulating sufficiency. Athens: Technical Chamber of Greece; 2010.

[16] 2009 ASHRAE HANDBOOK FUNDAMENTALS, American Society of Heating, Refrigerating and Air-Conditioning Engineers, Inc. 1791 Tullie Circle, N.E., Atlanta, GA 30329.

[17] European Commision Eurostat Statistics Explained. 2012.

[18] E. Kakaras, S. Karellas, P. Vourliotis, P. Grammelis, P. Pallis, E. Karampinis. Comparison of the cost of heating of various technologies. Athens: National Technical University of Athens, CPERI; 2013.

[19] A. Algieri, P. Morrone, Energetic analysis of biomass-fired ORC systems for micro-scale combined heat and power (CHP) generation. A possible application to the Italian residential sector. Applied Thermal Engineering, 71, 751 (2013).

[20] S.Quoilin, M. Broek, S.Declaye, P.Dewallef, V.Lemort. Techno-economic survey of organic rankine cycle (ORC) systems. Renewable and Sustainable Energy Reviews, 22, 168(2013).

[21] J. Bruno, J. Lopez-Villada, E. Letelier, S. Romera, A. Coronas.Modelling and optimisation of solar organic rankine cycle engines for reverse osmosis desalination. Applied Thermal Engineering, 28, 2212 (2008).

[22] S-H. Yang, J. Y. Rhee. Utilization and performance evaluation of a surplus air heat pump system for greenhouse cooling and heating. Applied Energy, 105, 244 (2013).

[23] N. Aste, R. Adhikari, M. Manfren. Cost optimal analysis of heat pump technology adoption in residential reference buildings. Renewable Energy, 60, 615(2013).